Supporting Information for

Original article

PRMT6 promotes tumorigenicity and cisplatin response of lung cancer through triggering 6PGD/ENO1 mediated cell metabolism

Mingming Sun[a,†], Leilei Li[b,†], Yujia Niu[c,†], Yingzhi Wang[a], Qi Yan[a], Fei Xie[a], Yaya Qiao[a], Jiaqi Song[a], Huanran Sun[a], Zhen Li[b], Sizhen Lai[d], Hongkai Chang[a], Han Zhang[a], Jiyan Wang[a], Chenxin Yang[d], Huifang Zhao[d], Junzhen Tan[d],Yanping Li[e], Shuangping Liu[f], Bin Lu[g,h], Min Liu[i], Guangyao Kong[j], Yujun Zhao[k], Chunze Zhang[l], Shuhai Lin[c,*], Cheng Luo[k,*], Shuai Zhang[d,*], Changliang Shan[a,k,*]

[a]*State Key Laboratory of Medicinal Chemical Biology, College of Pharmacy and Tianjin Key Laboratory of Molecular Drug Research, Nankai University, Tianjin 300350, China*

[b]*Biomedical Translational Research Institute, Jinan University, Guangzhou 510632, China*

[c]*State Key Laboratory of Cellular Stress Biology, Innovation Center for Cell Signaling Network, School of Life Sciences, Xiamen University, Xiamen 361102, China*

[d]*School of Integrative Medicine, Tianjin University of Traditional Chinese Medicine, Tianjin 301617, China*

[e]*Department of Pathology and Institute of Precision Medicine, Jining Medical University, Jining 272067, China*

[f]*Department of Pathology, Medical School, Dalian University, Dalian 116622, China*

[g]*Department of Biochemistry and Molecular Biology, School of Basic Medical Sciences, Hengyang Medical School, University of South China, Hengyang 421001, China*

[h]*School of Laboratory Medicine and Life Sciences, Wenzhou Medical University, Wenzhou 325035, China*

[i]*Institute of Biomedical Sciences, Shandong Provincial Key Laboratory of Animal Resistance Biology, Collaborative Innovation Center of Cell Biology in Universities of Shandong, College of Life Sciences, Shandong Normal University, Jinan 250014, China*

[j]*National Local Joint Engineering Research Center of Biodiagnostics and Biotherapy, the Second Affiliated Hospital of Xi'an Jiaotong University, Xi'an 710004, China*

[k]*State Key Laboratory of Drug Research, Shanghai Institute of Materia Medica, Chinese Academy of Sciences, Shanghai 201203, China*

[l]*Department of Colorectal Surgery, Tianjin Union Medical Center, Nankai University, Tianjin 300121, China*

Received 15 January 2022; received in revised form 26 April 2022; accepted 25 May 2022

*Corresponding authors.

E-mail addresses: changliangshan@nankai.edu.cn (Changliang Shan), shuaizhang@tjutcm.edu.cn (Shuai Zhang), cluo@simm.ac.cn (Cheng Luo), shuhai@xmu.edu.cn (Shuhai Lin).

[†]These authors made equal contributions to this work.

1. Supporting materials and methods

1.1. Colony formation

The cells were plated in 6-well plates for 800 cells and cultured for 2 weeks. The colonies were calculated after fixed and stained with 1% crystal violet. Colony number was measured by Image J.

1.2. Cell proliferation assay

Cell proliferation assays were performed by seeding 2×10^4 cells in 12-well plates. Cell growth was determined by cell numbers recorded at 0, 1, 2, 3 and 4 days after being seeded.

1.3. Cell viability assays

The H1299 and H460 cells were seeded in 96-well plates at 800 cells each well and incubated with increasing concentrations of inhibitors at 37 °C for indicated times. Relative cell viability at each experimental time point up to 72 h was determined by using MTT assay.

1.4. The shRNA-mediated gene silencing and viral infection

The short hairpin RNA (shRNA) plasmids targeting PRMT1, PRMT3, PRMT4, PRMT5 and PRMT6 were purchased from Transheep Biological Corporation (Transheep, Shanghai, China). To establish stable knockdown cells, the HEK293T cells were transfected with lentiviral shRNA constructs plus with viral packaging plasmids (psPAX2 and pMD2.G). The viral supernatant was collected and filtered through 0.45-μm filter after 3 days transfection. Then the H1299 and H460 cells were transduced by lentivirus and selected with 2 μg/mL puromycin. The knockdown efficacity was determined by Western blotting.

1.5. Plasmids cloned and transfections

Human PRMT1, PRMT3 and PRMT6 cDNA was cloned into pLVX3 for Flag-tag at N-terminus. Human PRMT4 cDNA was cloned into pEZ for Flag-tag at N-terminus. Human 6PGD cDNA was cloned into pDEST-GST for Flag-tag at N-terminus. 6PGD R324K was cloned into pDEST-GST for Flag-tag at N-terminus were performed using the Fast Mutagenesis System (TRAN, Beijing, China). Human 6PGD cDNA was cloned into pcDNA3.1 for Flag-tag at N-terminus. 6PGD R324K was cloned into pcDNA3.1 for Flag-tag at N-terminus were performed using the Fast Mutagenesis System. Human 6PGD cDNA was cloned into pGEX-4T for GST-tag at N-terminus. 6PGD R324K was cloned into

pGEX-4T for GST-tag at N-terminus were performed using the Fast Mutagenesis System. Human 6PGD cDNA was cloned into pETM3C for Flag-tag at N-terminus. 6PGD R324K was cloned into pETM3C for Flag-tag at N-terminus were performed using the Fast Mutagenesis System. Human ALDOA cDNA was cloned into pLVX3 for GST-tag at N-terminus. Human ENO1 cDNA was cloned into pLVX3 for GST-tag at N-terminus. R9K, R15K, R50K, R183K, R372K, R412K, and R9K/372K mutations were cloned into pLVX3 for GST-tag at N-terminus were performed using the Fast Mutagenesis System. Human ENO1 cDNA was cloned into pETM3C for GST-tag and Flag-tag at N-terminus. R9K, R15K, R50K, R183K, R372K, R412K, and R9K/372K mutations were cloned into pETM3C for GST-tag and Flag-tag at N-terminus was performed using the Fast Mutagenesis System. For transient transfections, cells were grown to 80% confluency and transfected with plasmids using polyethylenimine (PEI) Transfection Reagent (Polysciences, IL, USA) according to the manufacturer's protocol.

1.6. Quantitation of mRNA expression by quantitative real-time PCR (qRT-PCR)

Cells were washed with PBS and total RNA isolated with the Trizol reagent (Thermo Fisher Scientific, MA, USA), and then was subjected to reverse transcription using the PrimeScript RT reagent Kit (TaKaRa, Dalian, China) according to the manufacturer's instructions. qRT-PCR reactions were performed with the TB Green Premix Ex Taq (Takara, Dalian, China) on a CFX96™ real-time PCR detection system (Bio-Rad, CA, USA) and primers listed in Supplementary TABLE. Gene expression was calculated using the comparative $2^{-\Delta\Delta CT}$ method with the actin for normalization. All PCR runs were performed in triplicate and the data was analyzed by CFX Manager Software (Bio-Rad, CA, USA).

1.7. Seahorse assay

An XF-96 Extracellular Flux Analyzer (Seahorse Bioscience, Agilent Technologies, CA, USA) was used to analyze real-time bioenergetic status changes of the Extracellular acidification rate (ECAR) as described previously.

1.8. Histopathology and complete blood counts (CBC)

For histopathological analysis, sections of mouse tissue were stained with hematoxylin and eosin and slides were digitally scanned at 20 × magnification using a ScanScope XT from Aperio Technologies Inc. Imaged were analyzed and captured using ImageScope software (Aperio Technologies Inc, CA, USA) without any additional or subsequent image processing. For complete blood counts, blood was

collected retro-orbitally and immediately applied to a HemaVet 950FS (Drew Scientific Group, CT, USA) for generation of complete hematology profile.

1.9. Serum chemistry assays

For serum chemistry assays, blood was collected from mice retro-orbitally. Blood samples were incubated on ice for 2 h and centrifuged at 3000 rpm for 10 minutes (4 °C), then immediately applied to the following serum chemistry assays. The enzyme activity of alanine aminotransferase (ALT) in mouse serum was determined by measuring its product pyruvate in a reaction that concomitantly converts a nearly colorless probe to fluorescence (Ex/Em= 535/587) according to instruction of the Alanine Amiotransferase Activity Assay Kit (Biovision, CA, USA). The enzyme activity of aspartate aminotransferase (AST) in mouse serum was determined by measuring its product glutamate in a reaction that concomitantly converts a nearly colorless probe to color at 450 nm according to the instruction of Aspartate Aminotransferase Activity Assay Kit.

1.10. Immunohistochemical staining

Immunohistochemistry was performed on paraffin-embedded sections. Tissue sections were dewaxed and rehydrated using standard protocol. Antigen retrieval was performed by boiling samples in citrate buffer for 15 min. Endogenous peroxidase activity was inhibited by using 3% hydrogen peroxidase. Sections were blocked in 3% BSA in PBS and incubated in primary antibody (Ki67, or 6PGD, or ENO1, or PRMT6) overnight at 4 °C. Sections were rinsed in PBS and developed using 3,3′-diaminobenzidine (DAB). Sections were counterstained with hematoxylin. Quantification of staining was performed using Image J software.

1.11. Western blot analysis

Cells were lysed with NP40 lysis buffer (150 mmol/L NaCl, 10 mmol/L HEPES [pH=7.0], 1% NP40, 5 mmol/L $Na_4P_2O_7$, 5 mmol/L NaF, 2 mmol/L Na_3VO_4) containing protease inhibitor (complete ULTRA Tablets, Min, EDTA-free, EASYpack, Roche, BASEL, SWIT) on ice 30 min and then centrifuged at 12,000 rpm for 15 min at 4 °C. Protein samples were separated by 8% or 10% SDS-PAGE and transferred onto 0.2 μm or 0.45 μm PVDF membranes (Millipore, MA, USA) according to protein molecular mass. Firstly, the membranes were blocked with 5% non-fat milk for 2 h. Secondly, the membranes incubated overnight at 4 °C (or 2 h at room temperature) with the primary antibody. Thirdly,

the membranes incubated 1 h at room temperature with secondary antibody. Lastly, the signals were detected using Luminol substrate solution (Millipore, MA, USA).

1.12. Flag-pull down (GST-pull down) or immunoprecipitation assay

Cells were lysed in NP40 lysis buffer on ice 30 minutes and then centrifuged at 12,000 rpm for 15 min at 4 °C. Subsequently, the cell lysates were subjected to immunoprecipitation using different antibody-conjugated beads (Flag-conjugated beads or GST-conjugated beads), which were incubated overnight at 4 °C. Immune complexes were extensively washed for three times with cold TBS and analyzed by western blotting with specific antibodies.

1.13. Isotope tracing

Cells were incubated in RPMI 1640 media supplemented with dialyzed fetal bovine serum (Biological Industries, Israel) containing 11.11 mmol/L [1,2]^{13}C-glucose for the indicated duration, washed with room-temperature PBS, quenched with 1500 μL 80% LC–`MS grade methanol, then every sample was stored at –80 °C.

To measure glycolysis and pentose phosphate pathway, cells were subjected to three rapid freeze-thaw cycles, and then mixture was cooled (4 °C) for 1 h. The samples were vortexed and centrifuged for 15 min at 14,000 × *g* at 4 °C. The supernatant was pelleted by centrifugation at 4 °C and the supernatant containing aqueous metabolites was collected and evaporated to dryness using a SpeedVac concentrator. Metabolites were reconstituted in 60 μL of acetonitrile: water (1:1, *v*/*v*) with 0.1% formic acid vortexed and centrifuged to remove insoluble material.

The LC–MS system was performing using an Exion LC system (AB Sciex, MA, USA) with ZIC-pHILIC column (100 mm × 2.1 mm, Millipore, MA, USA) connected to QTRAP-5500 mass spectrometer (AB SCIEX, USA). For LC condition, 2 μL samples were injected and analyzed. The column rate is 0.2 mL/min. The column and tray temperature were set at 40 °C and 4 °C separately. Mobile phase A contains 15 mmol/L ammonium acetate, 3 mL/L ammonium hydrate (> 28%) in water and mobile phase B are 90% acetonitrile aqueous solution. The gradient elution was set as follows: 95% B maintained for 1 min, decreased to 45% over 14 min and held for 2 min, increased to 95% over 0.5 minute and remained for 4.5 min. The ESI voltage was set to 4500 V in negative ion MRM mode. Ion temperature and curtain gas were set at 500 °C and 35 μL/min. LC–MS/MS conditions were controlled by Analyst 1.7.1 software and the final data were processed by Mutiquant 3.0.3 software.

1.14. Data analysis

Natural-abundance correction of ^{13}C for tracer experiments was performed with AccuCor. The number of biological replicates in each experiment was listed in the figure legends. Statistical analyses of LC–MS data were described in the figure legends. Unless otherwise noted, statistically significant differences were assessed by a two-tailed paired *t* test. Graphing was done in Microsoft Excel and GraphPad Prism 8 (GraphPad Software Inc., Calif, USA).

2. Supporting figures

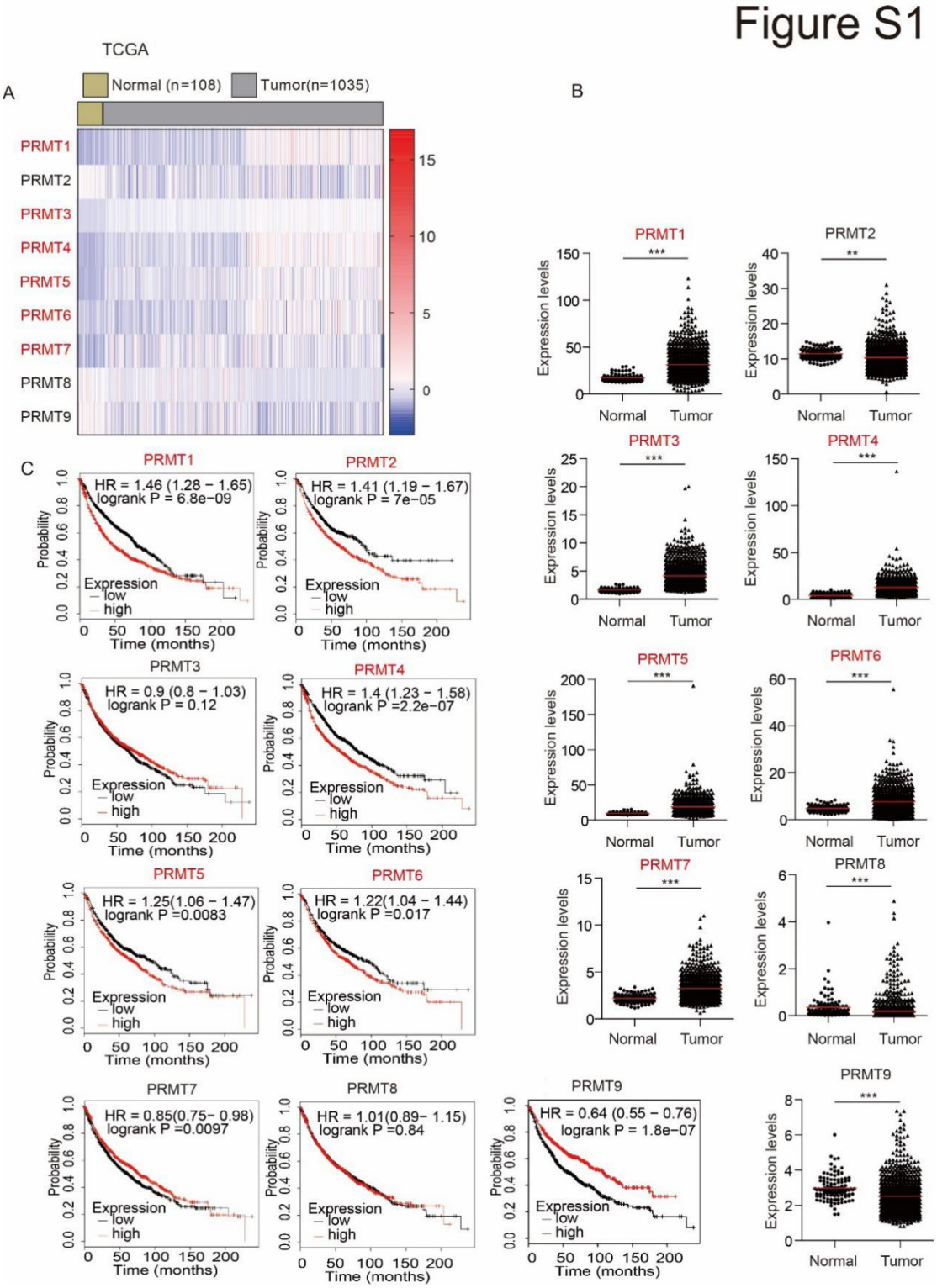

Figure S1 PRMT6 expression is elevated in lung cancer. (A) Heat map profiling the expression of PRMTs in the TCGA database of lung cancer. (B) The mRNA levels of PRMTs were analyzed between

lung cancer tissues and normal tissues from the GEO database. (C) Kaplan–Meier curves of overall survival in lung cancer patients with high and low expression of PRMTs, calculated from (http://kmplot.com/analysis/).

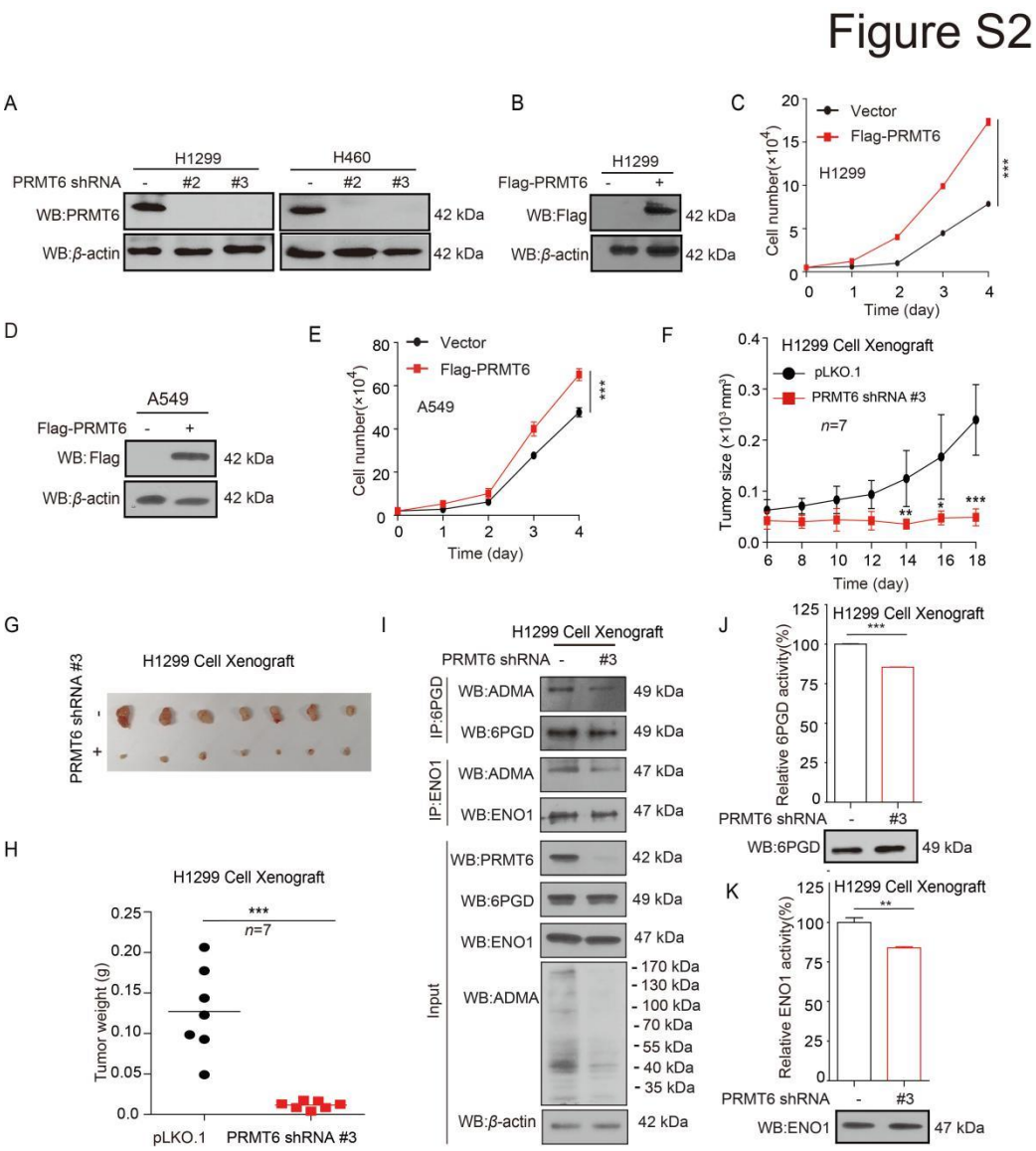

Figure S2 PRMT6 promotes lung cancer cell growth. (A) PRMT6 was determined by Western blotting in PRMT6 knockdown H1299 and H460 cells. (B) Western blotting analysis of PRMT6 protein expression in H1299 cells when expressed PRMT6. (C) Cell number counting assay was determined in human lung cancer H1299 cells with exogenous expressed PRMT6 (Data represent mean values ± SD from three independent experiments). (D) Western blotting analysis of PRMT6 protein expression in A549 cells when expressed PRMT6. (E) Cell number counting assay was determined in human lung

cancer A549 cells with exogenous expressed PRMT6 (Data represent mean values ± SD from three independent experiments). (F) Tumor growth was compared between xenograft nude mice injected with PRMT6 knockdown H1299 cells and control vector cells (n=7). (G) All tumors from nude mouse are shown. (H) Tumor mass in xenograft nude mice injected with PRMT6 knockdown H1299 cells compared to mice injected with the control vector cells (n=7). (I) The arginine methylation levels of 6PGD/ENO1 and 6PGD/ENO1 were analyzed by immunoprecipitation assay (IP) in a representative PRMT6 knockdown H1299 tumor. (J) 6PGD enzyme activities were analyzed in a representative PRMT6 knockdown H1299 tumor (The data represent mean values ± SD from three replicates of each sample). (K) ENO1 enzyme activities were analyzed in a representative PRMT6 knockdown H1299 tumor (The data represent mean values ± SD from three replicates of each sample). (*P < 0.05; **P < 0.01; ***P < 0.001).

Figure S3

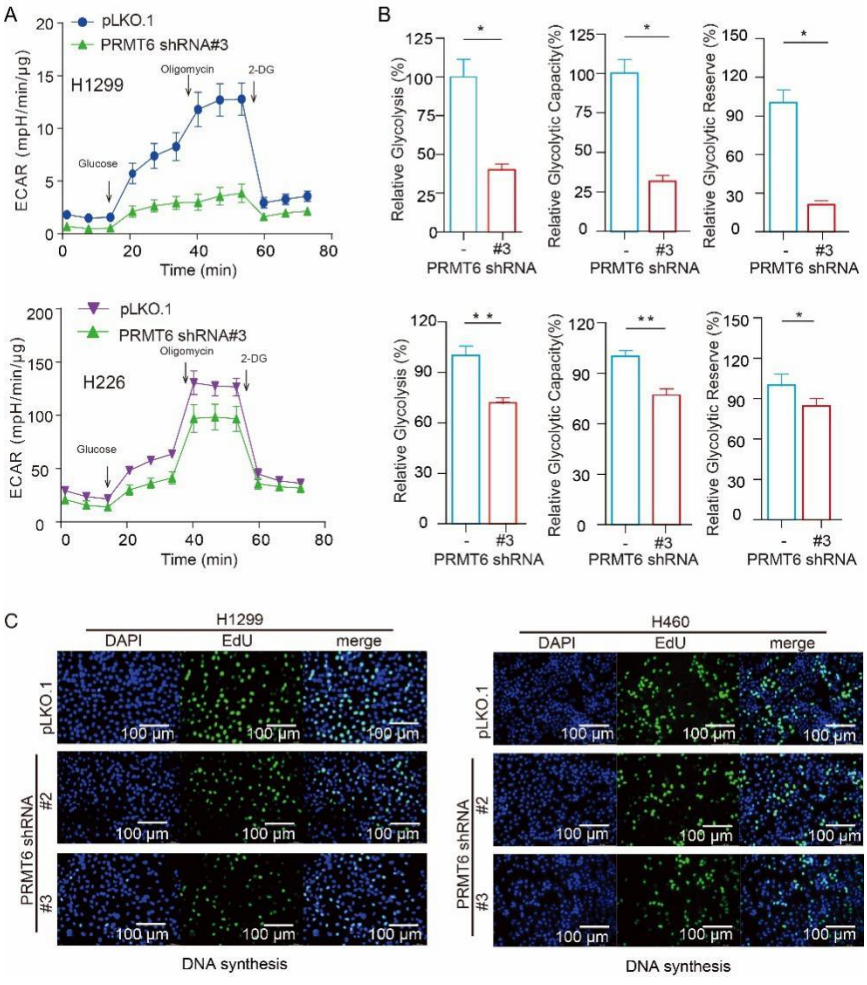

Figure S3 PRMT6 promotes oxidative PPP flux and glycolysis pathway. (A, B) ECAR rate (a proxy for the rate of glycolysis) was determined by using a Seahorse 96XF extracellular flux analyzer following sequential addition of glucose (11 mmol/L), oligomycin (1.0 μmol/L), and 2-DG (100 mmol/L), as indicated by arrows, in PRMT6 knockdown H1299 and H226 cells. (C) The DNA synthesis was determined by using EdU incorporation assay in PRMT6 knockdown cells. The data represent mean values ± SD from three independent experiments (* $P < 0.05$; ** $P < 0.01$; *** $P < 0.001$).

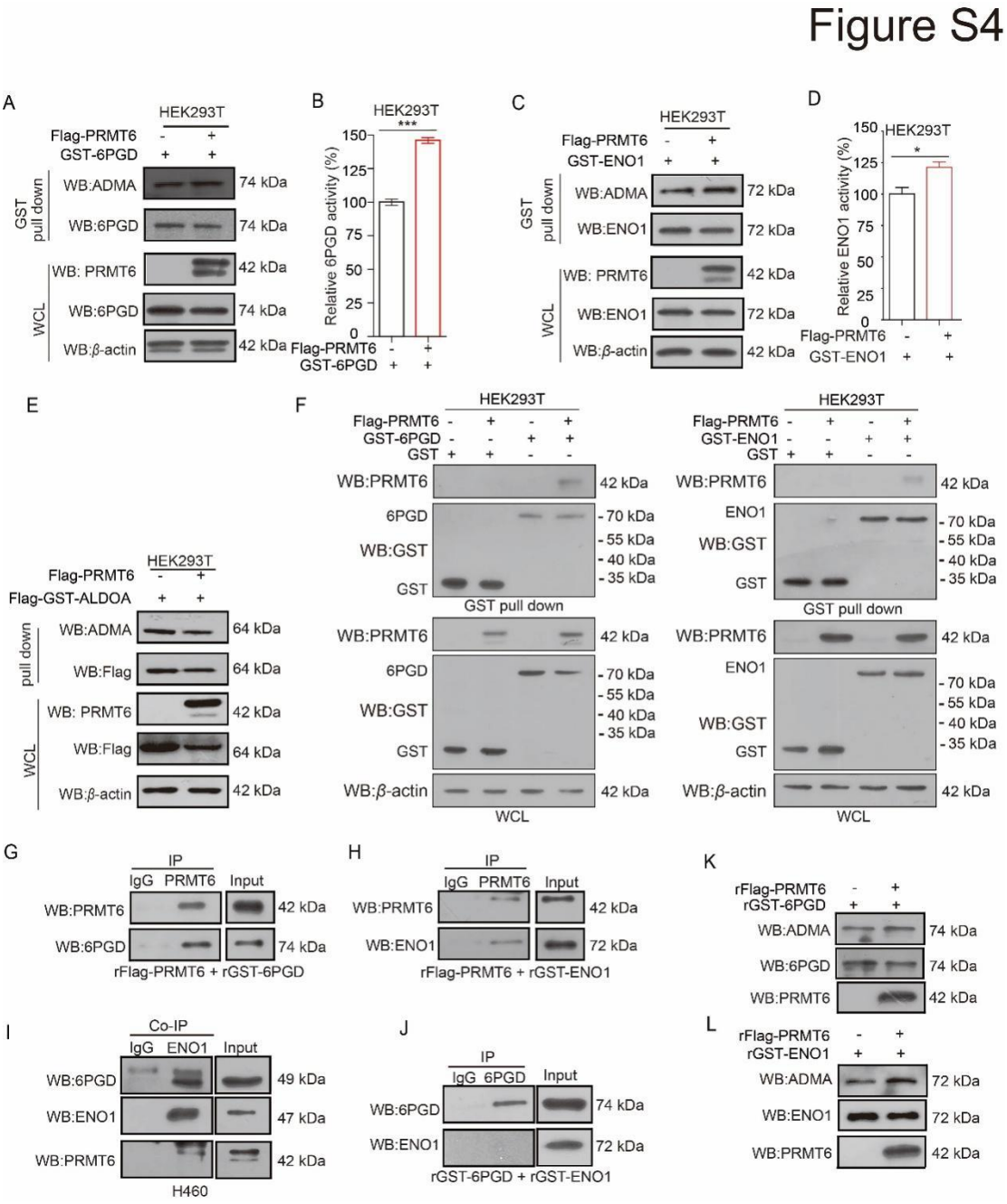

Figure S4 PRMT6 methylates 6PGD/ENO1 and enhances their activities. (A) GST-pull down of 6PGD from HEK293T cells, which co-express GST-6PGD with or without Flag-PRMT6, followed by Western blotting to detect the ADMA levels of 6PGD. (B) GST-pull down of 6PGD from HEK293T cells, which co-express GST-6PGD with or without Flag-PRMT6, followed by the enzyme activity assay to detect the 6PGD enzyme activity. (C) GST-pull down of ENO1 from HEK293T cells, which co-express GST-ENO1 with or without Flag-PRMT6, followed by Western blotting to detect the ADMA levels of ENO1. (D) GST-pull down of ENO1 from HEK293T cells, which co-express GST-ENO1 with or without Flag-PRMT6, followed by the enzyme activity assay to detect the ENO1 enzyme activity. (E) GST-pull down of ALDOA from HEK293T cells, which co-express GST-ALDOA with or without Flag-PRMT6, followed by Western blotting to detect the ADMA levels of ALDOA. (F) GST-pull down of 6PGD from HEK293T cells, which co-express GST-6PGD (or GST-ENO1) with or without Flag-PRMT6, followed by Western blotting to detect PRMT6 and 6PGD (or ENO1). (G) 6PGD associates with PRMT6 *in vitro*. The rFlag-PRMT6 protein was incubated with rGST-6PGD. After Co-Immunoprecipitation (Co-IP), the interaction between rFlag-PRMT6 protein and rGST-6PGD was analyzed by Western blotting. (H) ENO1 associates with PRMT6 *in vitro*. The rFlag-PRMT6 protein was incubated with rGST-ENO1. After Co-Immunoprecipitation (Co-IP), the interaction between rFlag-PRMT6 protein and rGST-ENO1 was analyzed by Western blotting. (I) Co-IP was applied to analyze the interaction between 6PGD and ENO1 by Western blotting in H460 cells. (J) ENO1 associates with 6PGD *in vitro*. The rGST-6PGD protein was incubated with rGST-ENO1. After Co-IP, the interaction between rGST-ENO1 protein and rGST-6PGD was analyzed by Western blotting. (K) Purified rGST-6PGD was incubated with purified rFlag-PRMT6 from bacterica, followed by Western blotting to detect the ADMA levels of 6PGD. (L) Purified rGST-ENO1 was incubated with purified rFlag-PRMT6 from bacterica, followed by Western blotting to detect the ADMA levels of ENO1. The data represent mean values ± SD from three replicates of each sample (*$P < 0.05$; **$P < 0.01$; ***$P < 0.001$).

Figure S5

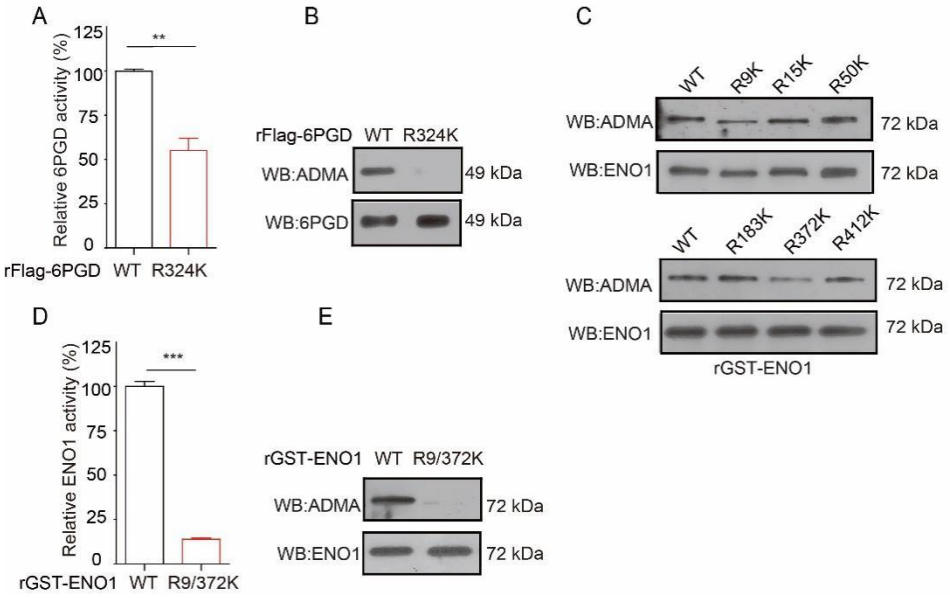

Figure S5 PRMT6 regulates 6PGD and ENO1 activity by methylating their R324 and R9/372 sites. (A) Purified rFlag-6PGD WT and rFlag-6PGD R324K were analyzed for 6PGD enzyme activity. (B) Purified rFlag-6PGD WT and rFlag-6PGD R324K were analyzed by Western blotting to detect the ADMA levels. (C) Purified rGST-ENO1 WT, R9K, R15K, R50K, R183K, R372K, and R412K were analyzed ADMA levels by Western blotting. (D) Purified rGST-ENO1 WT and R9/372K were analyzed for ENO1 enzyme activity. (E) Purified rGST-ENO1 WT and R9/372K were analyzed by Western blotting to detect the ADMA levels. The data represent mean values ± SD from three replicates of each sample (*$P < 0.05$; **$P < 0.01$; ***$P < 0.001$).

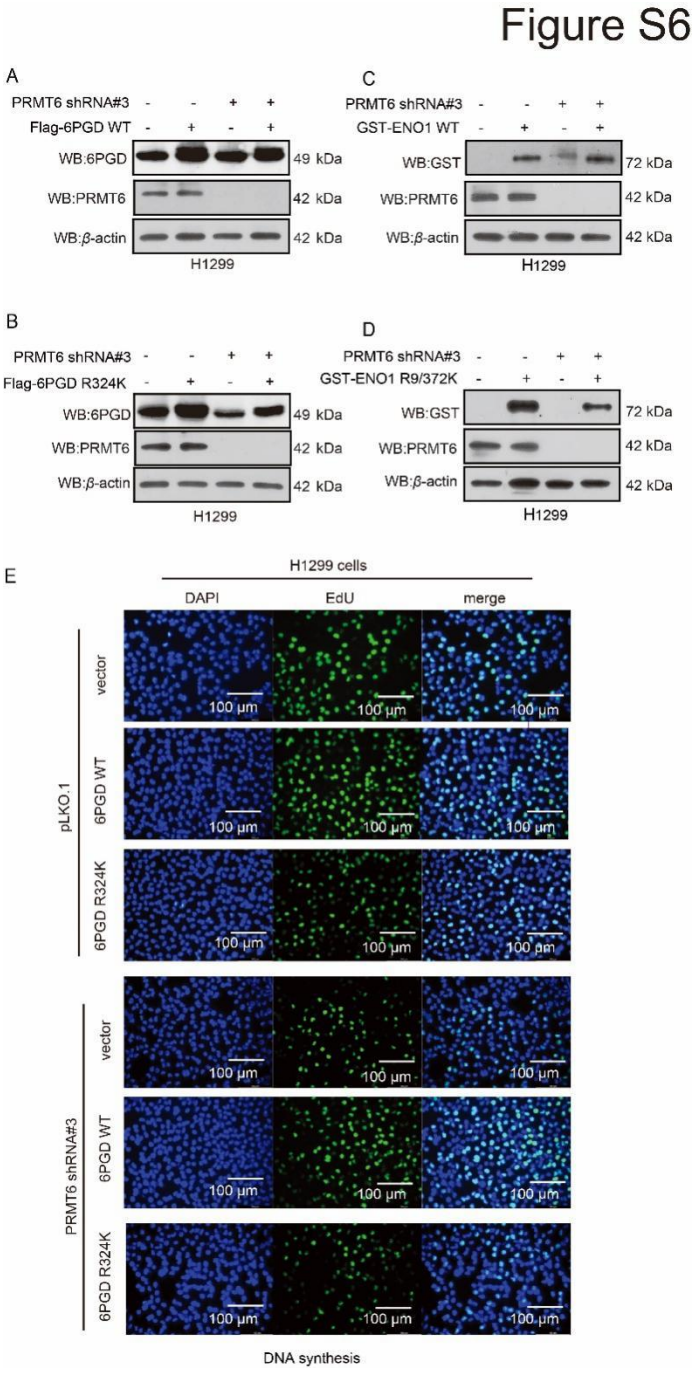

Figure S6 PRMT6 enhances oxidative PPP flux, glycolysis pathway, and cell proliferation by activating 6PGD and ENO1. (A) Western blotting analysis of 6PGD and PRMT6 in PRMT6 knockdown cells with or without exogenously expressing 6PGD WT. (B) Western blotting analysis of 6PGD and PRMT6 in PRMT6 knockdown cells with or without exogenously expressing 6PGD R324K. (C) Western blotting analysis of ENO1 and PRMT6 in PRMT6 knockdown cells with or without exogenously expressing ENO1 WT. (D) Western blotting analysis of ENO1 and PRMT6 in PRMT6

knockdown cells with or without exogenously expressing ENO1 R9/372K. (E) DNA synthesis was determined by using EdU incorporation assay in stable knockdown of PRMT6 cells with or without exogenously expressing 6PGD WT or R324K.

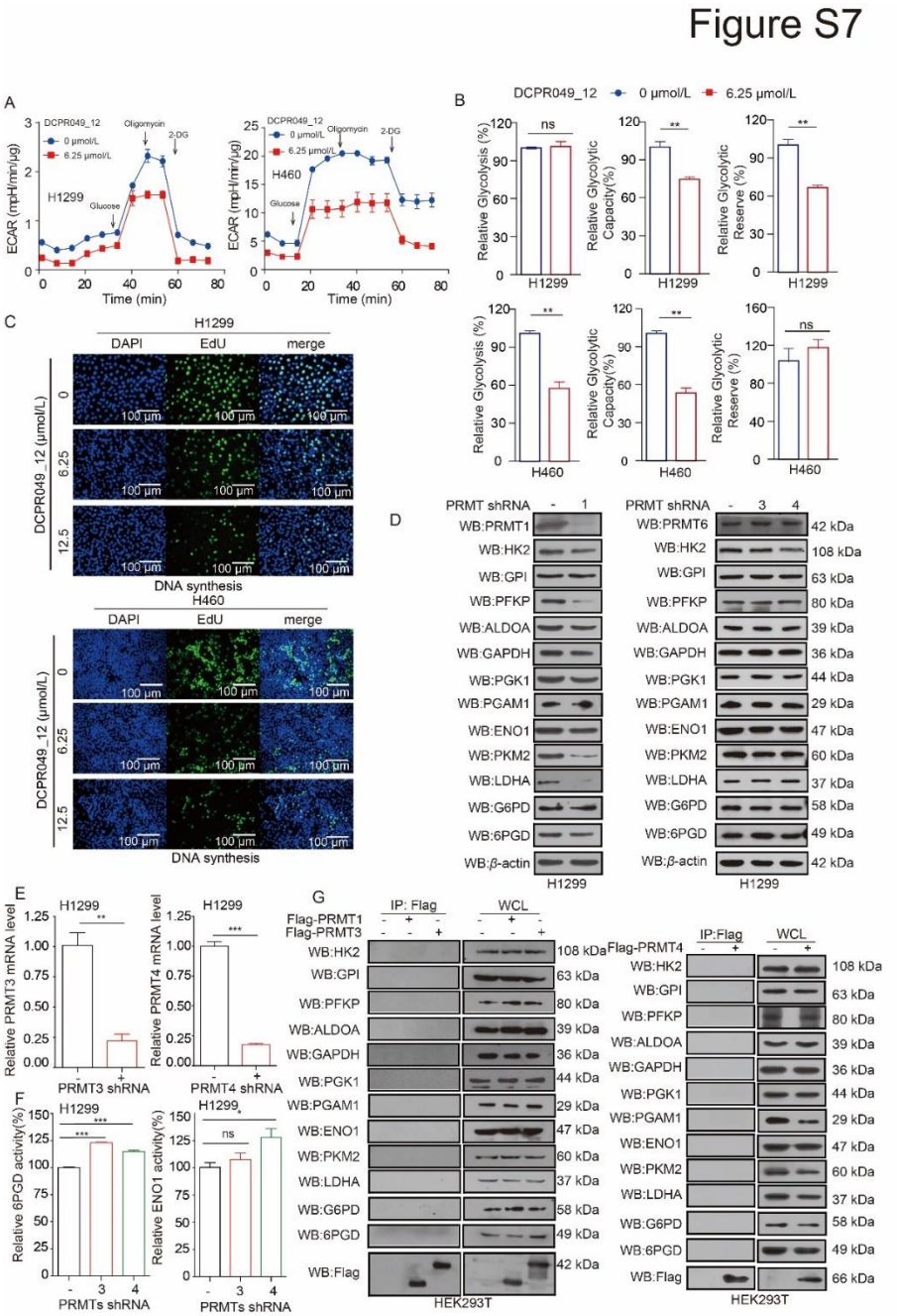

Figure S7 DCPR049_12 inhibits the oxidative PPP flux and glycolysis pathway by regulating activities of 6PGD and ENO1. (A, B) ECAR rate (a proxy for the rate of glycolysis) was determined by using a Seahorse 96XF extracellular flux analyzer following sequential addition of glucose (11 mmol/L),

oligomycin (1.0 μmol/L), and 2-DG (100 mmol/L), as indicated by arrows, in H1299 and H460 cells treated with or without DCPR049_12. (C) The DNA synthesis was determined by using EdU incorporation assay in H1299 and H460 cells treated with or without DCPR049_12. (D) The expression of glycolysis-, and oxidative PPP-related enzymes were determined by Western blotting in PRMT1, PRMT3 and PRMT4 knockdown H1299 cells. (E) PRMT3 and PRMT4 mRNA levels were determined by qRT-PCR in PRMT3 and PRMT4 knockdown H1299 cells. (F) The enzyme activities of 6PGD and ENO1 were determined in PRMT3 and PRMT4 knockdown H1299 cell by activity assay. (G) The expressions of glycolysis-, and PPP-related enzymes were determined by Western blotting in HEK293T cells by Flag-pull down assay. The data represent mean values ± SD from three independent experiments (*$P < 0.05$; **$P < 0.01$; ***$P < 0.001$).

Figure S8

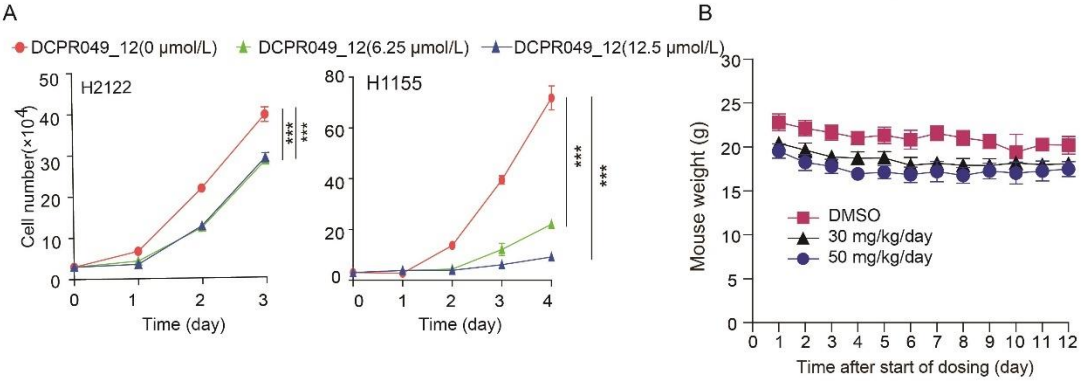

C

Test Name	Normal range	DMSO (mean)	30 mg/kg/day (mean)	50 mg/kg/day (mean)
ALT (U/L)	17-77	44 ± 14.0	31.5 ± 4.9	70.7 ± 43
AST (U/L)	54-298	135 ± 9.6	128 ± 12.7	135.3 ± 46.2

D

Test Name	Normal range	DMSO (mean)	30 mg/kg/day (mean)	50 mg/kg/day (mean)
WBC (x 10^3/mL)	2.6-10.1	5.3 ± 0.2	4.5 ± 2.0	6.8 ± 3.3
LYM (x 10^3/mL)	1.3-8.4	4.5 ± 0.7	1.9± 1.0	3.0± 1.1
MONO (x 10^3/mL)	0-0.3	0.0 ± 0.0	0.0 ± 0.005	0.04 ± 0.03
HCT (%)	32.8-48	39.1 ± 6.9	39.8 ± 4.4	34.9 ± 4.0
MCV (fl)	42.3-55.9	48.5 ± 0.3	46.9 ± 0.7	47.8 ± 1.8
RDWa (%)	0-99.9	13.6 ± 0.5	14.6 ± 0.9	17.0 ± 2.7
HGB (g/dl)	10-16.1	13.0 ± 2.4	13.3 ± 1.9	11.4 ± 1.0
MCHC (g/dl)	29.5-35.1	33.2 ± 0.5	33.2 ± 1.2	32.7 ± 0.8
RBC (x 10^6/mL)	6.5-10.1	8.1 ± 1.4	8.5 ± 1.1	7.3 ± 0.7
MCH (pg)	13.7-18.1	16.1 ± 0.2	15.6 ± 0.4	15.6 ± 0.4
PLT (x 10^3/mL)	250-1540	506.7 ± 135.6	827.0 ± 125	879 ± 87.7
MPV (fl)	0-99.9	7.2 ± 0.2	6.7 ± 0.2	7.0 ± 1.2

Figure S8 DCPR049_12 suppresses the lung cancer cell growth. (A) Cell proliferation was determined by cell number counting assay in lung cancer cells treated with DCPR049_12. (B) Effects of

chronic treatment with DCPR049_12 or DMSO on body weights of nude mice. (C) Effects of chronic treatment with DCPR049_12 or DMSO on serum chemistry of nude mice are shown. ALT: alanine aminotransferase; AST: aspartate aminotransferase. (D) Peripheral blood samples from DCPR049_12 or DMSO-treated nude mice (3 representative mice) were examined for hematological properties using CBC analysis. The data represent mean values ± SD from three independent experiments (*$0.01 < P < 0.05$; **$0.001 < P < 0.01$; ***$P < 0.001$).

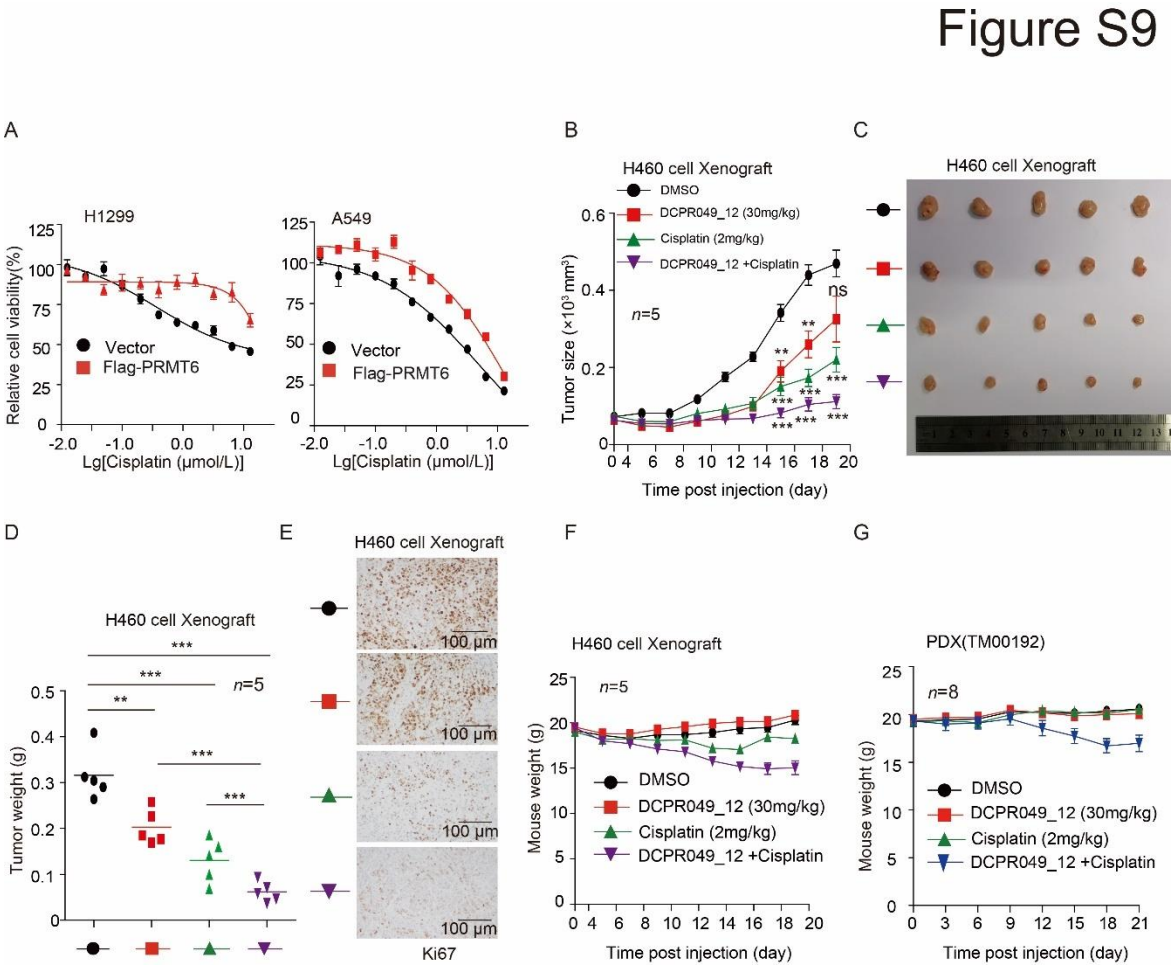

Figure S9 DCPR049_12 enhances anti-tumor effect of cisplatin. (A) Cell proliferation rates were determined by MTT in H1299 and A549 cells with overexpression of PRMT6 when treated with or without cisplatin. Each bar represents mean± SD (n = 8). (B) Tumor growth was compared between xenograft nude mice injected with H460 cells treated with DCPR049_12 alone, cisplatin alone, and combination (n = 5). (C) All tumors from nude mouse are shown. (D) Tumor mass in xenograft nude mice injected with H460 cells treated with DCPR049_12 alone, cisplatin alone, and combination (n = 5).

(E) Ki67 was analyzed in a representative H460 tumor treated with DCPR049_12 alone, cisplatin alone, and combination by IHC. (F) Effects of chronic treatment on body weights of H460 xenograft nude mice with DCPR049_12 alone, cisplatin alone, and combination ($n = 5$). (G) Effects of chronic treatment on body weights of PDX xenograft nude mice with DCPR049_12 alone, cisplatin alone, and combination ($n = 8$). (*$P < 0.05$; **$P < 0.01$; ***$P < 0.001$).

3. Supporting tables

Table S1 key resources.

REAGENT or RESOURCE	SOURCE	IDENTIFIER
Antibodies		
PRMT1 Rabbit PolyAb	proteintech	11279-1-AP
PRMT6 Rabbit PolyAb	proteintech	15395-1-AP
G6PD Rabbit mAb	proteintech	25413-1-AP
6PGD Rabbit mAb	proteintech	14718-1-AP
PFKP Rabbit mAb	proteintech	13389-1-AP
LDHA Rabbit mAb	proteintech	19987-1-AP
PKM2 Rabbit Ab	proteintech	15822-1-AP
PGAM1 Rabbit PolyAb	proteintech	16126-1-AP
GPI Rabbit PolyAb	proteintech	15171-1-AP
ENO1 Rabbit PolyAb	proteintech	11204-1-AP
ALDOA Rabbit PolyAb	proteintech	11217-1-AP
GAPDH Mouse MAb	proteintech	60004-1-Ig
HK2 Rabbit PolyAb	proteintech	22029-1-AP
PGK1 Rabbit PolyAb	proteintech	17811-1-AP
Bata Actin Mouse McAb	proteintech	66009-1-Ig
Ki67 Rabbit PolyAb	CST	9027S
Flag Rabbit PolyAb	proteintech	20543-1-AP
Flag Mouse PolyAb	proteintech	66008-3-Ig
Symmetric Di-Methyl Arginine Motif [sdme-RG] MultiMab™ Rabbit mAb mix	Cell signaling	13222S
Asymmetric Di-Methyl Arginine Motif [adme-R] MultiMab™ Rabbit mAb mix	Cell signaling	13522S
GST Antibody	Cell signaling	2625S
Biological Samples		
Lung Cancer patients sample (Cohort 1)	The First Affiliated Hospital of Wenzhou Medical University	N/A
Lung Cancer patients sample (Cohort 2)	Shanghai Outdo Biotechnology	N/A
Bacterial and Virus Strains		
Trans10 Chemically Competent Cell	TransGen Biotech	Cat# CD101-01
Trans BL21(DE3) Chemically Competent Cell	TransGen Biotech	Cat# CD601-03
Chemicals, Peptides, and Recombinant Proteins		
DCPR049_12	This paper	N/A

Cisplatin	MedChemExpress	HY-17394
2-Phosphoglycerate	Shanghai yuanye Bio-Technology Co., Ltd	70195-25-4
ADP	Sigma	20398-34-9
NADH	Sigma	606-68-8
PKM2/LDHA	Sigma	P0294
6-PG	Sigma	P7877
$NADP^+$	Sigma	N5755
3 × Flag peptide	APExBIO	A6001
Protein G sepharose	GE Healthcare Life Sciences	17-0618-01
Trizma base	Sigma-Aldrich	V900483
SAM	Sigma	A4377
Anti-Flag agarose affinity gel	Sigma-Aldrich	A4596
Polyethylenimine (PEI)	Polysciences	23966
Polybrene	Sigma	H9268
Puromycin	InvivoGen	Ant-pr-1
TRIzol	Thermo Fisher Scientific	15596018
Methanol	CNW	CAEQ-4-000306-4000
Acetonitrile	CNW	CAEQ-4-003306-4000
L-Serine	Sigma	56-45-1
L-Phenylalanine (RING-D5, 98%)	Cambridge Isotope Laboratories	DLM-1258-PK
D-Glucose (1,2-13C2, 99%)	Cambridge Isotope Laboratories	CLM-504-PK
DMEM Medium	Thermo Fisher Scientific	C11995500BT
RPMI 1640 Medium, no glucose	BasalMedia	H430827
RPMI 1640 Medium, no Phenol Red	Thermo Fisher Scientific	11835-030

Critical Commercial Assays

TB Green® Premix Ex TaqTMII(Tli RNaseH plus)	TaKaRa	RR820A
TransStart FastPfu DNA Polymerase	TransGen Biotech	AP221-12
Fast mutagenesis system	TransGen Biotech	FM111-01
Endo-free plasmid maxi kit	Omega	D6926-03
EasyPure plsmid miniprep kit	TransGen Biotech	EM101-02
Seahorse XF glycolytic rate assay kit	Seahorse Bioscience, Agilent Technologies	103344-100
Cell-LightTM Edu Apollo488 In Vitro Kit	RIBOBIO	C10310-3
Lactate Assay Kit	Nanjing Jiancheng Bioengineering Institute	A019-2-1
Aspartate Aminotransferase Activity	Biovision	K753-100

(AST) Assay Kit		
Alanine Aminotransferase (ALT) Activity Colorimetric Assay Kit	Biovision	K752-100
NADP+/NADPH Assay Kit with WST-8	Beyotime	S0179
Reative Oxygen Species Assay Kit	Beyotime	S0033
Experimental Models: Cell Lines		
HEK293T	This paper	N/A
H1299	This paper	N/A
H226	This paper	N/A
H460	This paper	N/A
H157	This paper	N/A
A549	This paper	N/A
BEAS-2B	This paper	N/A
H2122	This paper	N/A
H1944	This paper	N/A
H1155	This paper	N/A
H1437	This paper	N/A
shRNA		
pLKO.1-puro	TranSheepBio	N/A
pLKO.1-puro-PRMT1#1-#3	TranSheepBio	N/A
pLKO.1-puro-PRMT3#1-#3	TranSheepBio	N/A
pLKO.1-puro-PRMT4#1-#3	TranSheepBio	N/A
pLKO.1-puro-PRMT5#1-#3	TranSheepBio	N/A
pLKO.1-puro-PRMT6#1-#3	TranSheepBio	N/A
Oligonucleotides		
Primer (qPCR) PRMT3-F	5′-AAGAAAGCAGTTATTCCAGAAGC-3′	N/A
Primer (qPCR) PRMT3-R	5′-CCCGTAGAGAACACGACCC-3′	N/A
Primer (qPCR) PRMT4-F	5′-AGTGGACCTGTCGGCCCTCC-3′	N/A
Primer (qPCR) PRMT4-R	5′-ATCCTGTGCAAATCTCCTTCTTTGG-3′	N/A
Recombinant DNA		
pLVX3-PRMT1	This paper	N/A

pLVX3-PRMT3	This paper	N/A
pEZ-Flag-PRMT4	This paper	N/A
pLVX3-PRMT6	This paper	N/A
pDEST27-GST-Flag-6PGD	This paper	N/A
pDEST27-GST-Flag-6PGD R324K	This paper	N/A
pCDNA3.1-Flag-6PGD	This paper	N/A
pCDNA3.1-Flag-6PGD R324K	This paper	N/A
pGEX-4T1-Flag-6PGD	This paper	N/A
pGEX-4T1-Flag-6PGD R324K	This paper	N/A
pETM3C-GST-6PGD	This paper	N/A
pETM3C-GST-6PGD R324K	This paper	N/A
pLVX3-GST-ALDOA	This paper	N/A
pLVX3-GST-ENO1	This paper	N/A
pLVX3-GST-ENO1 R9K	This paper	N/A
pLVX3-GST-ENO1 R15K	This paper	N/A
pLVX3-GST-ENO1 R50K	This paper	N/A
pLVX3-GST-ENO1 R183K	This paper	N/A
pLVX3-GST-ENO1 R372K	This paper	N/A
pLVX3-GST-ENO1 R412K	This paper	N/A
pLVX3-GST-6PGD R324K	This paper	N/A
pLVX3-GST-ENO1 R9K/R372K	This paper	N/A
pETM3C-GST-ENO1	This paper	N/A
pETM3C-GST-ENO1 R9K	This paper	N/A
pETM3C-GST-ENO1 R15K	This paper	N/A
pETM3C-GST-ENO1 R50K	This paper	N/A
pETM3C-GST-ENO1 R183K	This paper	N/A
pETM3C-GST-ENO1 R372K	This paper	N/A
pETM3C-GST-ENO1 R412K	This paper	N/A
pETM3C-GST-ENO1 R9K/R372K	This paper	N/A

Software and Algorithms

GraphPad Prism 8	Graph- Pad	Graph- Pad
Adobe Illustrator	Adobe	Adobe
ImageJ	National Institutes of Health	National Institutes of Health
Leica Application Suite X -2.0.1	Leica Microsystems	N/A
FlowJo-10	FlowJo	N/A
Compusyn	Chou TC.2010	N/A

Table S2 Expression of PRMT6 protein in non-small cell lung cancer (NSCLC).

Diagnosis	No. of case	PRMT6				Positive cases rate (%)	Strong positive cases rate (%)
		–	+	++	+++		
NSCLC	41	2	18	21	0	95.1%***	**51.2%***
Adjacent normal lung	41	17	22	2	0	58.6%	4.9%

Positive rate: percentage of positive cases with +, ++, and +++ staining score.

Strongly positive rate (high-level expression): percentage of positive cases with ++ and +++ staining score.

****P* < 0.001 compared with adjacent normal lung.

Table S3 Relationship between PRMT6 protein overexpression and the clinicopathological features of non-small cell lung cancer (NSCLC).

Variables	No. of case (*n*)	PRMT6 strong positive rate (%)	*P* value
Gender			
Male	30	18 (60.0%)	0.1822
Female	11	5 (45.5%)	
Age (years)			
> 62	16	9 (56.3%)	0.9717
≤ 62	25	14 (56.0%)	
Tumor size			
≤ 4 cm	21	12 (57.1%)	0.327
＞ 4cm	20	11 (55.0%)	
TNM stage			
I–II	21	10 (47.6%)	0.3245
II–III	20	13 (65.0%)	